Tribological behavior of electric vehicle transmission oils using Al_2O_3 nanoadditives

José M. Liñeira del Río[a,b]*, Enriqueta R. López[a], Josefa Fernández[a]

[a]*Laboratory of Thermophysical and Tribological Properties, Nafomat Group, Department of Applied Physics, Faculty of Physics, and Institute of Materiais (iMATUS), Universidade de Santiago de Compostela, 15782, Santiago de Compostela, Spain*

[b]*Unidade de tribologia, vibraçoes e manutençao industrial, INEGI, Universidade do Porto, Porto, Portugal*

*Corresponding author.

E-mail address: josemanuel.lineira@usc.es (José M. Liñeira del Río)

ABSTRACT: Antifriction and antiwear performances of Al_2O_3 nanoparticles (NPs) as additives of an automatic transmission fluid, ATF are presented in this research. For this purpose, four nanodispersions were formulated: ATF + 0.05 wt% Al_2O_3 NPs, ATF + 0.10 wt% Al_2O_3 NPs, ATF + 0.15 wt% Al_2O_3 NPs and ATF + 0.20 wt% Al_2O_3 NPs to identify the optimal concentration of additive. Tribological experiments were taken at pure sliding conditions, with the formulated nanolubricants and the ATF, under a working load of 20 N. The four nanolubricants tested resulted in lower friction coefficients than those obtained using ATF, reaching a maximum reduction of 6% with the ATF + 0.10 wt% Al_2O_3 nanolubricant. The tribological pairs tested with the Al_2O_3 nanolubricants show lower wear than those tested with the ATF, having the best wear decrease with the ATF + 0.10 wt% Al_2O_3 nanolubricant, with reductions of 45, 57 and 78%, respectively, in diameter, depth and area of the wear scar. Furthermore, by means of confocal Raman microscopy, roughness evaluation and SEM-EDX of the worn tribological specimens, it can be determined that mending, tribo-sintering as well as rolling mechanisms occur.

Keywords: ATF oil; electric vehicles; tribological mechanisms; friction; wear.

1. INTRODUCTION

The demand for energy is growing rapidly, which raises concerns about the impact on the natural environment and climate change. However, not all the energy consumed in the world goes to cover this demand since, despite the significant advances in friction and wear control, friction consumes about a fifth of the energy used worldwide, with transportation in the lead [1].

In this scenario, the electric vehicle (EV) is a promising solution, since friction losses in internal combustion engine (ICE) cars roughly double those in electric cars [1]. It is known that just 20% from the total fuel energy supplied to an ICE vehicle is used to push the vehicle whereas an EV uses about 80% from the electric energy from the grid. Thus, EV is almost four times more efficient than an ICE when the electrical energy comes from renewable sources [1,2]. Even though EVs are very efficient in terms of energy consumption, there is still much to be done to further improve efficiency, for which the challenge is to minimize friction and wear. In addition, one of the main advantages of the EVs is their great capability to reduce greenhouse gas emissions [3]. These gas reductions, particularly of carbon dioxide, CO_2, strongly depend on the source of the electricity [1]. Thus, when electricity comes from renewable energy sources, the CO_2 emissions of an EV are 4.5 times lower than those of a combustion engine car [1]. Hence, EVs being very efficient and producing very few gas emissions, the difficulties of their efficiency and resistance of EVs affect the mobile components and, therefore, their tribology. Thus, tribological solutions such as new materials or optimized lubricants can help to increase the driving range of EVs by reducing friction in elements such as gears or bearings. In some type of EVs, the electric motor (EM) and power electronics are inside the transmission housing, operating the mechanical elements of EVs at higher speeds, loads and temperatures than in ICEs, and under electromagnetic conditions [4,5]. Therefore, low viscosity lubricants are needed as transmission fluids of the electrified drivetrains owing to the high torque and operational speeds of tribological elements in EVs [5]. These specific lubricants are called electric transmission fluids (ETFs) [5,6]. By decreasing the viscosity of the oil, viscous drag and viscous heating reduce and heat transfer is improved [4,7]. Nevertheless, if the lubricant viscosity is reduced, boundary lubrication can appear that leads to severe tribological contact. This fact implies that enhanced antiwear and antifriction lubricant properties are necessary.

In this vein, nanotechnology is included among the new technologies that have benefited friction research [1,8]. Thus, the use of nanomaterials as lubricant additives can help to develop new low-viscosity lubricants particularly adapted to the necessities of the electric drivetrains as they are promising antiwear and antifriction additives and, consequently, an extended motor life could be achieved under severe operational conditions and hard lubrication systems [9]. In addition, many nanoparticles (NPs) are more environmentally friendly than traditional additives [10,11].

Nanoadditives have shown good achievements improving the antifriction and antiwear capabilities of traditional lubricants [12-17]. However, the research on nanolubricants in relation to the EVs' tribological requirements is scarce. Recently, Mustafa et al. [4] reviewed some low-viscosity lubricants, focusing on polyalphaolefins (PAO) due to their high-performance as gear base oils and hydro lubricants.

Given these demands, it is necessary to study potential lubricants based on low-viscosity oils and nanoadditives. In this work, the main objective is to study the tribological properties of aluminum oxide (Al_2O_3) nanoparticles as additives of a low-viscosity oil specific for automatic transmissions, ATF. The current standard for electrified transmission lubricants are automatic transmission fluids (ATFs), because some properties such as efficiency, durability, seal compatibility or wide operating range of ETFs are common to those of ATFs [9]. In this work, the main objective is to study the tribological properties of aluminum oxide nanoparticles (Al_2O_3 NPs) as additives of a formulated ATF. According to the manufacturers, this lubricant guarantees silent operation in automatic boxes, allows smooth gear to change due to the friction stability, and has good oxidation resistance and thermal stability. In this vein, García Tuero et al. [3] analyzed the tribological performance of a commercial ATF using a phosphonium-based ionic liquid ($[P_{6,6,6,14}]$[BEHP]) as additive reaching good antiwear results. Regarding the Al_2O_3 NPs, different studies have shown good tribological results [18-20]. For instance, Ghalme et al. [19] analyzed the effect of the addition of Al_2O_3 NPs (50 nm) as lubricant additives on the tribological performance of SAE10W40 obtaining reductions in wear scar diameter and friction coefficient of 21% and 23% respectively with the addition of 0.5 wt% of Al_2O_3 NPs. The authors concluded that the lubrication performance was improved due to mending and ball bearing effects of Al_2O_3 NPs. Furthermore, Luo et al. [20] measured the tribological properties (friction and wear) of a lubricating oil with Al_2O_3/TiO_2 nanocomposites modified with KH-560 (75 nm) as additive, observing a much better tribological performance in comparison to lubricant base oil, being the tribological mechanism due to protective film formation on the rubbed surface and sliding friction changing to rolling friction during the rubbing process [18]. Moreover, Gundarneeya and Vakharia [21] found that incorporating Al_2O_3 NPs (20 nm) as lubricant additives into Avalon ISO Viscosity grade 46 oil, led to a higher maximum pressure and load carrying capacity of the journal bearing in comparison to the oil without NPs. Finally, Nabhan et al. [22] examined the tribological performance of hybrid MWCNTs/Al_2O_3 NPs as additives of a 10W30 engine oil. These authors found that the coefficient of friction and wear scar width were enhanced by around 48% and 52%, respectively, when compared to unmodified oil.

In literature there are many articles on Al_2O_3 NPs as lubricant additives, obtaining good tribological performance. Most of these papers primarily focus on the use of Al_2O_3 NPs in biodiesel fuels to enhance engine performance [23,24] , in the design of nanofluids for minimal quantity of lubrication for the metal cutting industries [25] or in automotive combustion engine oils [26]. However, no studies have investigated the effect of Al_2O_3 NPs as additives on low viscosity oils (kinematic viscosity at 100 °C<10 cSt) which is a key factor in the development of ETFs. Only Peña-

Parás et al. [18] includes a low viscosity oil, Polyalphaolefin 8 (8 cSt at 100 °C), which is suitable as base oil for ETFs, but the morphology of their NPs is tubular. In addition, the article does not report information about the stability of the nanolubricants, and the NPs size is not specifically indicated (<50 nm). In contrast, the ATF (6.20 cSt at 100 °C) used in this work is a specially formulated low viscosity oil with an additive package (antifriction, antiwear, among other additives), making it exceedingly challenging to enhance its lubrication properties, and the Al_2O_3 NPs are spherical (5.5 nm average diameter).

2. Material and methods

2.1. Materials

ATF is a low viscosity lubricant for automatic transmissions of electric vehicles, designed to protect gear and gearbox bearings from wear and corrosion, with improved oxidation stability and good dielectric properties. This ATF is formulated with around 90 wt% of API G-III synthetic base oils and 10 wt% of an additive package. This lubricant has a dynamic viscosity and density at 313.15 K of 31.21 mPa·s and 0.8271 g·cm^{-3}, respectively, as well as a 152 viscosity index.

Gamma Al_2O_3 NPs (γ-Al_2O_3), with an average size of 5 nm and purity >99%, were supplied by US Research Nanomaterials, Inc. (Houston, TX USA). γ-Al_2O_3, is one of the forms of transition aluminas, which are obtained from the thermal treatment of aluminium hydroxides [27]. Scanning electron microscopy (SEM, Zeiss FESEM Ultra Plus) and transmission electron microscopy (TEM, JEOL 1011) techniques were used to characterize the shape and size of the Al_2O_3 NPs. SEM and TEM images (Fig. 1) show that these NPs present a nearly spherical shape.

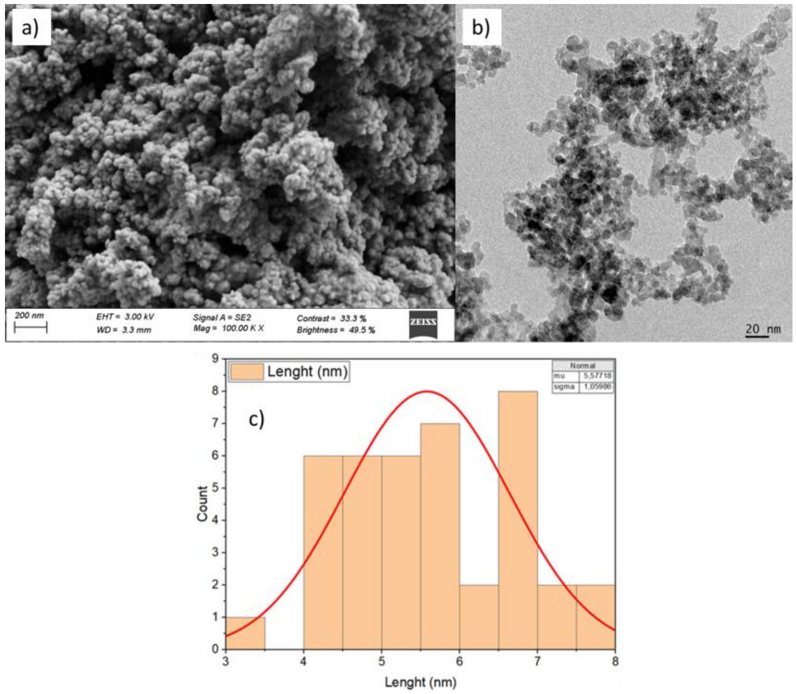

Fig. 1 SEM (a) and TEM (b) images and NPs size distribution (c) of Al_2O_3 NPs.

Regarding the nanoparticle sizes, Fig. 1c shows the size distribution of Al_2O_3 NPs (obtained with ImageJ), observing that the average sizes for the NPs are around 5.5 nm, which agrees with the information provided by the manufacturer (5 nm).

Moreover, the Al_2O_3 NPs were also characterized by infrared spectroscopy (FTIR) to identify the chemical bonds as well as functional groups of the nanoparticles (Fig. 2a). In this spectrum, the absorption peaks at 3457 and 1643 cm^{-1} can be assigned to the stretching and bending vibrations of adsorbed water molecules and the stretching of the framework Al–OH group with the defective sites [28]. This is coherent with the fact of the chemical composition of the transition alumina is that of aluminium oxide, with a residual content of hydroxyl groups depending on the dehydroxylation of the aluminium hydroxides [27,29]. Furthermore, the observed peaks at 813, 755, and 512 cm^{-1} for the vibrations of Al–O–Al in Fig. 2 proves the γ-form of Al_2O_3 NPs [28,29].

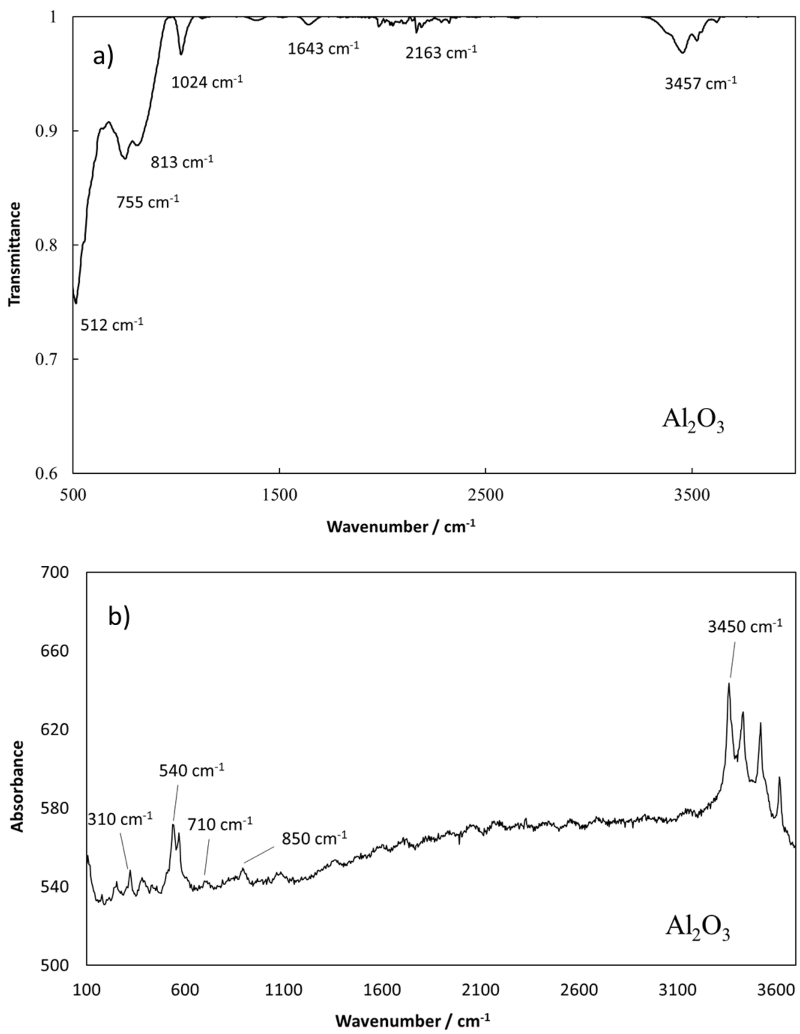

Fig. 2 FTIR (a) and Raman (b) spectra of Al_2O_3 NPs.

Regarding the Raman characterization of Al_2O_3 NPs, the spectrum (Fig. 2b) displays several bands in the region of 100–3600 cm^{-1} with an absorbance maximum at 3450 cm^{-1} attributed to stretching vibrations in absorbed water molecules [30]. Fig. 2b also shows that the bands have different intensities and non-elementary shapes. The sharp peaks in the 200–850 cm^{-1} region with significant bands at 310, 415, 540, 710 and 850 cm^{-1} correspond to vibrations of the Al–O bond in the tetrahedral structure of AlO_4 [30,31]. The presence of this structure in bulk γ-Al_2O_3 though Raman spectra was identified previously [30,31].

2.2. Nanodispersions formulation

Nanolubricants were designed by means of the traditional two-step method (Fig. 4). Dry Al_2O_3 NPs were blended with ATF using a Sartorius balance (readability of 0.01 mg) to determine the nanolubricant mass concentrations. Subsequently, the blend homogenization was carried out through an ultrasonic bath. The sonication duration is four hours, with temperature control throughout the procedure. The bath water is replaced about every hour when the temperature reaches around 45 °C. Using the previous method, different masses of Al_2O_3 NPs were added in the ATF to obtain the follow nanodispersions: ATF + 0.05 wt% Al_2O_3, ATF + 0.10 wt% Al_2O_3, ATF + 0.15 wt% Al_2O_3 and ATF + 0.20 wt% Al_2O_3.

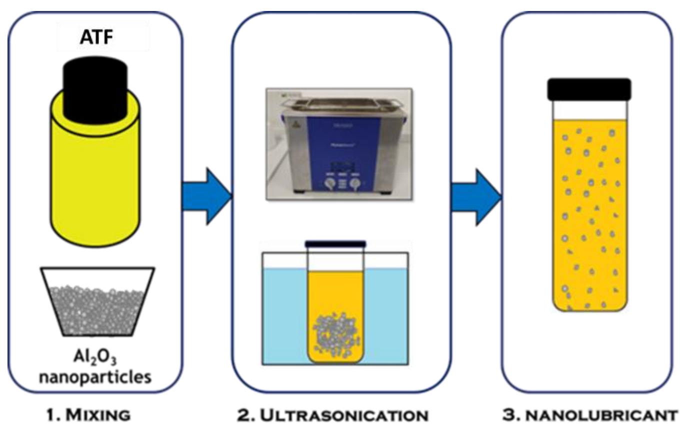

Fig. 3. Scheme of two-step preparation method.

After the preparation of nanolubricants, their stability times were evaluated through the visual control, taking photos of the unaltered nanodispersions each day until the precipitation of the Al_2O_3 NPs. As can be observed in Fig. 4, NPs start to sediment 14 days after the nanolubricant preparation, especially in the case one with the highest concentration, 0.20 wt% Al_2O_3 NPs. This time is much longer than the time needed to carry out the tribological tests: friction and wear analysis. For comparison, we have included in Fig. 4 photos of the nanodispersion containing the base oil of the ATF (API G-III) and 0.05 wt% Al_2O_3 NPs. As can be observed, sedimentation of the Al_2O_3 NPs is evident eight hours after its preparation.

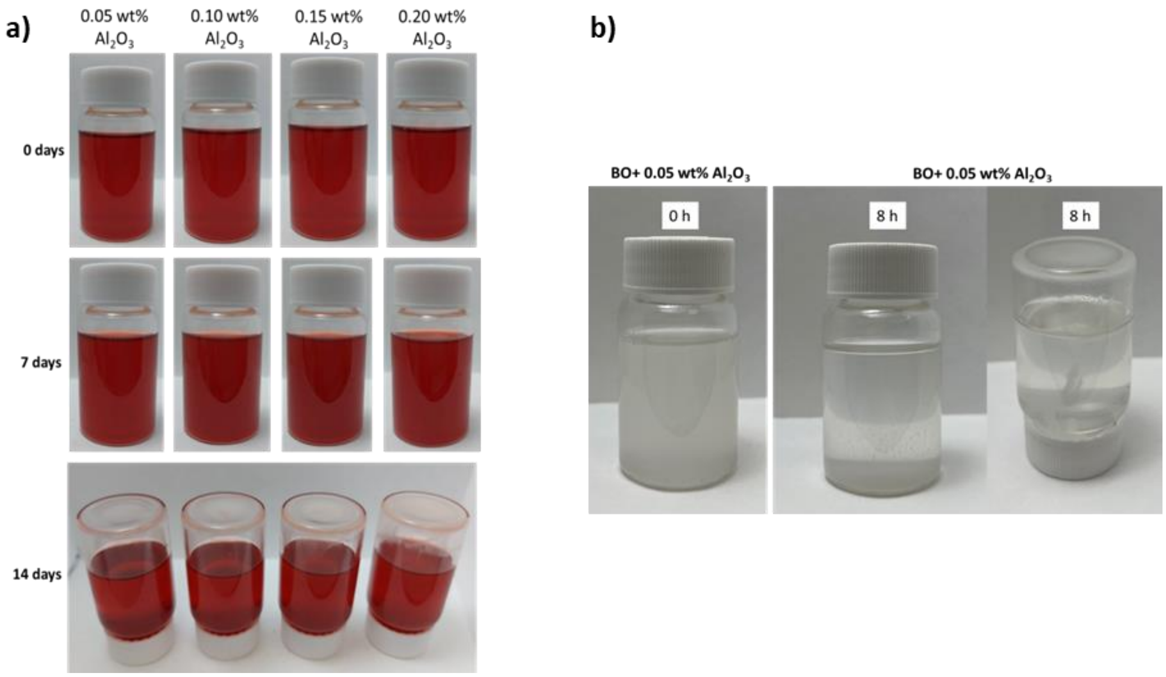

Fig. 4. Visual observation of a) ATF nanolubricants containing Al_2O_3 NPs, b) base oil (API G-III) of ATF with 0.05 wt% Al_2O_3.

Furthermore, to complete the stability analysis of the nanolubricants, the refractive index for the 0.05 wt% Al_2O_3 nanolubricant (based on ATF) at 298.15 K was the measured together with that for the dispersion of Base oil API G-III + 0.05 wt% Al_2O_3 to know if this additive package of the ATF plays a role in achieving a good stability. For this aim, a Mettler Toledo RA-510M refractometer was used. Fig. 5 displays the evolution of the refractive index for both Al_2O_3 nanolubricants with an NPs concentration of 0.05 wt%. After the initial ten hours, the refractive index of the Base oil + 0.05 wt% Al_2O_3 nanolubricant reaches a constant value, i.e., the NPs are fully sedimented. However, the NPs sedimentation in the ATF + 0.05 wt% Al_2O_3 nanolubricant occurs gradually. Specifically, for the first nanolubricant, refractive index increased by 0.27% after 10 hours, while for the ATF nanolubricant, the refractive index only increased by 0.07%. Therefore, it is suggested that the additive package in ATF lubricants has a positive effect on the stability of Al_2O_3 nanolubricants.

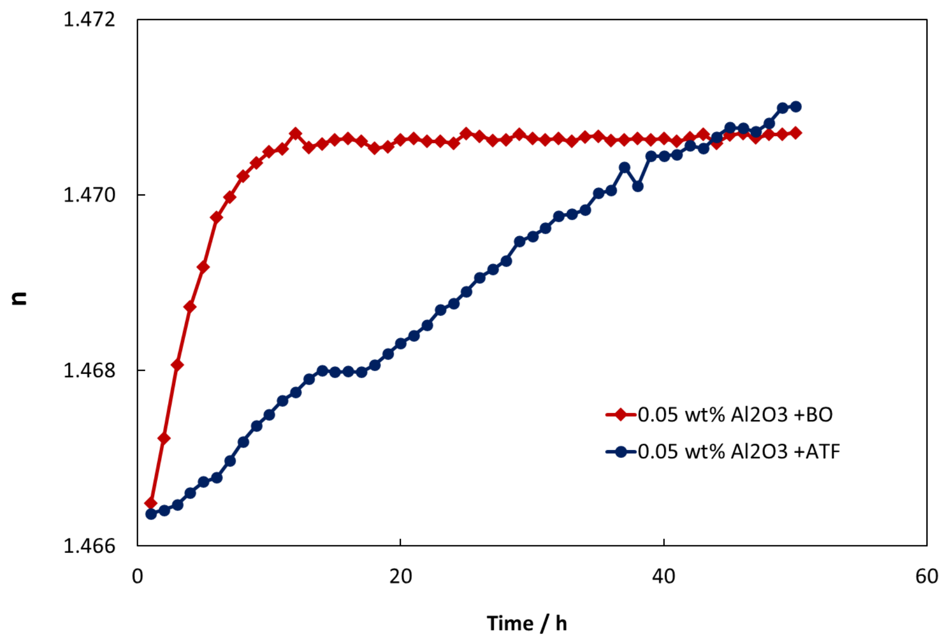

Fig. 5 Refractive index evolution for Al_2O_3 nanolubricants.

2.3. Friction tests and wear evaluation

Tribological studies with ATF and nanolubricants were performed using a T-PTD200 tribology cell coupled to a rheometer MCR 302, Anton Paar (Graz, Austria), in a ball-on-three pins geometry. The steel ball is fixed in a rotating tube that is driven by the rheometer. The pins form an angle of 135° with respect to the tube and are located inside a thermostated container. In each tribological test, the ball rotates on the three pins under a force applied by the rheometer. This axial force is transferred, giving rise to three normal forces perpendicular to each pin surface. More details can be found in [32-34]. For this work, cylindrical pins of 6x6 mm and 12.7 mm diameter balls both made of hardened 100Cr6 steel and with a hardness of 62-66 Rockwell C, were used. The tests were performed at 213 rpm rotational speed (0.1 m s^{-1} at the contact points) and 20 N axial load, equally distributed on the three pins (9.43 N on each pin) implying a maximum Hertzian pressure of 1.1 GPa, a duration of 3400 s and a temperature of 393.15 K. As the performance of electric motors improves, the power density increases, with a consequent increase in heat generation in the coil, and the resulting increase in temperature. In addition, to avoid demagnetization, the temperature must be below 423.15 K [35], thus effective motor cooling is crucial. As a result, to meet the cooling requirements, different approaches have been proposed. Among them, for high-power motors, liquid cooling is one of the most promising cooling techniques. Thus, the temperature was chosen 393.15 K according with previous results on the literature [36], in which the maximum motor temperature is close. More information regarding this tribological device can be found in a previous work [34].

Once the friction experiments have been carried out with each of the formulated Al_2O_3 nanolubricants and the ATF (at least 3 replicates of each one), the wear caused on each of the pins is evaluated to establish which of the nanolubricants has the best anti-wear performance. For this purpose, a 3D profiler (Sensofar S neox) was utilized to quantify the generated wear using different wear parameters: wear scar diameter (WSD), wear track depth (WTD) and worn area. The S neox 3D profiler was calibrated and verified by the manufacturer, following the ISO 25178 standard. These wear parameters were evaluated on the three pins tested with each nanolubricant to obtain suitable average values. The 3D profiler was also used to determine the wear track roughness (Ra and Rq) of the worn pins to illustrate the antiwear ability of each nanolubricant. For this task, ISO4287 standard was used, making use of a Gaussian filter (cut-off: 0.08 mm wavelength). In addition, SEM-EDX microscopy was also used to observe the worn surfaces of pins tested with all the formulated nanolubricants and the ATF and to obtain information on chemical composition of the worn track. Finally, a confocal Raman microscope from WITec was used to examine the worn surfaces of pins and reveal information about the NPs in the worn track and the possible tribological mechanisms that may have taken place.

3. Results and analysis

3.1. Friction and wear results

Fig. 6 and Table 1 present the mean friction coefficients (μ) for the ATF and base oil and its nanolubricants containing Al_2O_3 NPs at a temperature of 120 °C. It is clearly observed that the four nanolubricants have friction coefficients slightly lower than that of the ATF. In particular, the lowest μ value is obtained with the nanolubricant ATF + 0.10 wt% Al_2O_3 NPs, i.e., the optimum concentration of the Al_2O_3 NPs is 0.10 wt%, being the friction reduction 6 %. Additionally, Fig. 7 which displays the evolution of friction coefficient values during time, also shows that the nanolubricant ATF + 0.10 wt% Al_2O_3 NPs present the lowest friction results.

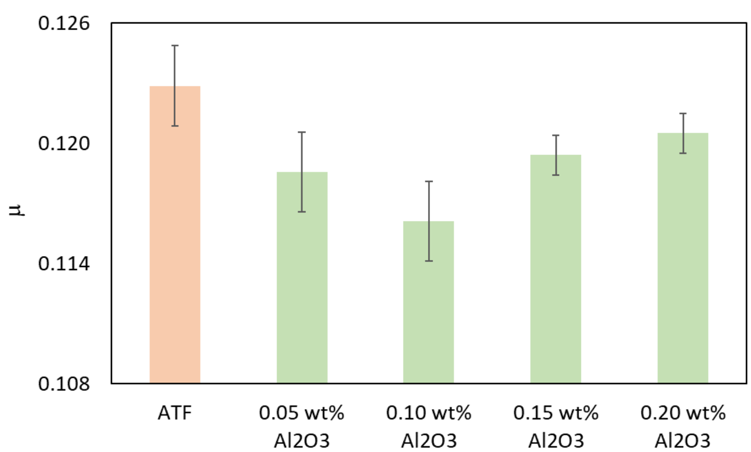

Fig. 6 Comparison between the average friction coefficients (μ) found with ATF and its nanolubricants containing Al_2O_3 NPs.

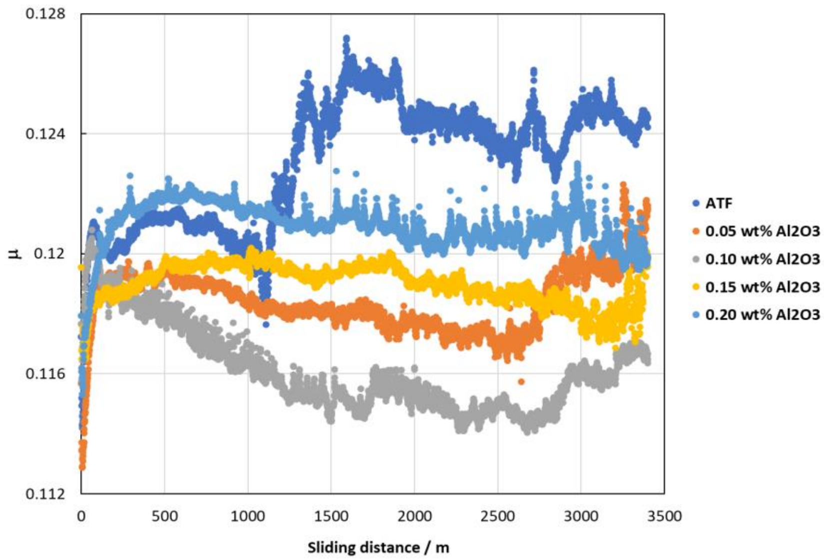

Fig. 7 Evolution of friction coefficient values for ATF and its nanolubricants containing Al_2O_3 NPs with the sliding distance at 120 ^oC.

Table 1

Average friction coefficients, μ, and average wear parameters with their standard deviations for the tested ATF lubricants.

Lubricant	μ	σ	WSD/μm	σ/μm	WTD/μm	σ/μm	Area/ μm^2	σ/ μm^2
ATF	0.123	0.002	289	16	0.82	0.09	163	27
+ 0.05 wt% Al_2O_3 NPs	0.119	0.002	202	16	0.49	0.07	89.1	16
+ 0.10 wt% Al_2O_3 NPs	0.116	0.002	158	11	0.35	0.04	35.5	10
+ 0.15 wt% Al_2O_3 NPs	0.120	0.001	209	18	0.49	0.08	81.1	17
+ 0.20 wt% Al_2O_3 NPs	0.121	0.001	219	15	0.35	0.14	93.1	14

As indicated previously, the wear generated during the tribological experiments was analyzed by means of the wear track parameters: diameter, depth and worn area. The values of WSD, WTD and worn area observed on the worn pins lubricated with the tested ATF dispersions are summarized in Table 1. All the wear parameters analyzed (Fig. 8 and Table 1) indicate that using the nanolubricants with Al_2O_3 NPs, the wear created during friction tests is much lower than that obtained with ATF. As with antifriction performance, it should be emphasized that the mass concentration of additives significantly affects antiwear performance. The wear results obtained have a similar trend with the values obtained for the friction coefficient (Fig. 6) Thus, the largest wear reductions in diameter, depth and area were also found with the nanolubricant ATF+ 0.10 wt% Al_2O_3 NPs, with reductions of 45, 57 and 78%, respectively. This phenomenon may be due to at very low concentrations (0.05 wt%) the content of NPs is not sufficient and when the concentration of additives is higher (0.15 and 0.20 wt%), NPs are more likely to agglomerate during friction tests, making it difficult for the NPs to enter the tribological contact region, causing poorer lubrication performance. Optimal concentrations for the tribological properties of many nanodispersions have been found previously [24,37-40], including some containing Al_2O_3 NPs [24,37]. For another spherical nanomaterials (ZrO_2/SiO_2 composite NPs) Zheng et al. [41] explain this phenomenon indicating that when less nanoparticles than the corresponding to the optimal concentration were added the friction zone could not be completely filled. Therefore, the ball bearing effect cannot play, and the anti-friction effect was not obvious. When more NPs were added the NPs were sintered into blocks by friction. Therefore, larger nanoparticles (aggregates) as impurities scratched the friction surface and the friction coefficient increased. Therefore, only when the added amounts of nanoparticles were in the optimal concentration range, the friction-reducing effect is better. Furthermore, for non-spherical NPs as reduced graphene oxide nanosheets, this phenomenon also occurs, which is explained by the existence of a point of saturation for the filling of the nanosheets into the friction zone [38].

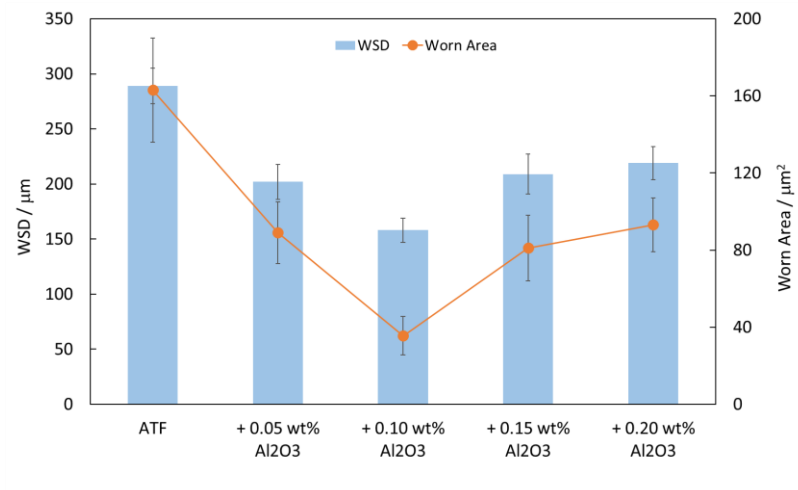

Fig. 8 Mean WSD and worn areas achieved with ATF and with its nanolubricants with Al_2O_3 NPs.

A comparison of the cross-sectional profiles and a 3D mapping of worn surfaces lubricated with ATF and its nanolubricants with Al_2O_3 NPs is presented in Fig. 9, in where the significant wear reductions can be observed when nanolubricants are used instead ATF.Therefore, with low concentrations of Al_2O_3 nanoadditives considerable antiwear improvements can be observed. These results are very important because the ATF is a formulated oil with an additive package (antifriction, antiwear, among others) and therefore it is very difficult to improve its lubrication properties as it was done in this work.

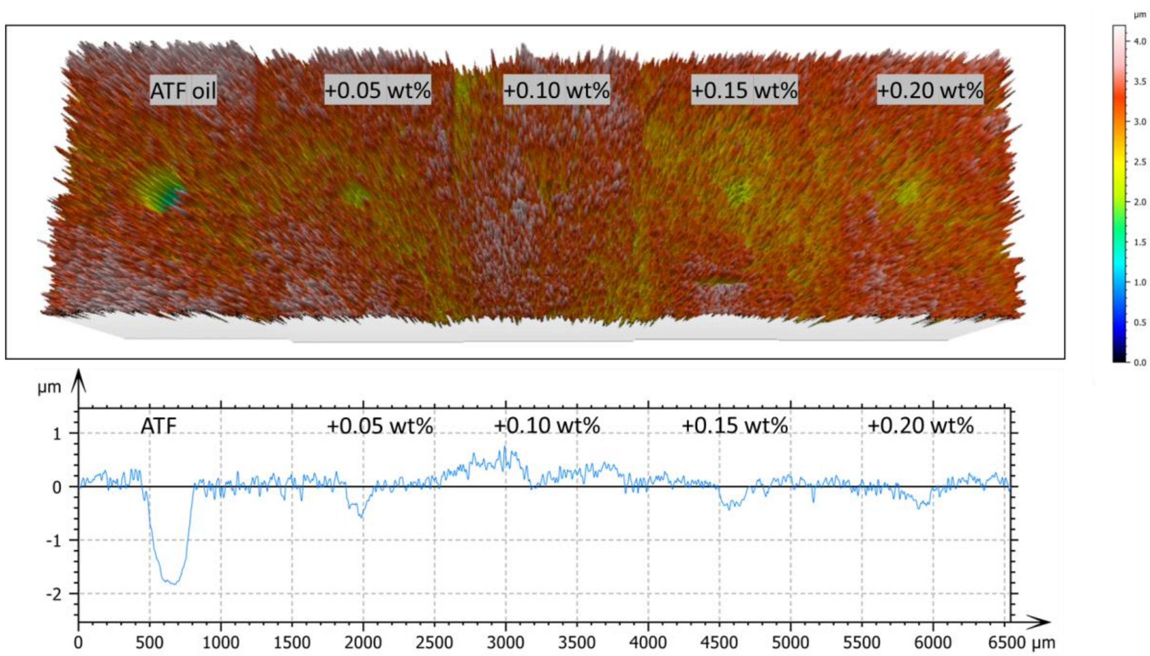

Fig. 9 3D Surface topography and cross-sectional profiles comparison of worn surfaces lubricated with ATF and with its nanolubricants containing Al_2O_3 NPs.

3.2. Tribological mechanisms discussion

To understand the tribological mechanism that could describe the better antifriction-antiwear behavior of nanolubricants compared to ATF, roughness analysis, Raman mapping, SEM microscopy and EDX analysis were carried out on the worn surfaces lubricated with the ATF and the nanolubricants with Al_2O_3 NPs.

Measurements of roughness (Ra and Rq) on worn pins reveal that the worn surfaces lubricated with nanolubricants containing Al_2O_3 NPs present lower roughness compared to those lubricated with ATF (Table 2). Thus, a Ra value of 18.8 nm was reached for the worn pins lubricated with ATF whereas for the those tested with the nanolubricant ATF + 0.10 wt% Al_2O_3 NPs the lowest Ra value (11.9 nm) was reached implying a roughness reduction of 37%. These roughness results showed that due to the presence of the NPs in the contact, a more regular surface is found after tribological tests.

Table 2
Mean roughness values, Ra and Rq with their uncertainties, σ, in worn pins tested with ATF lubricants.

Lubricant	Ra/nm	σ	Rq/ nm	σ
ATF	18.8	1.8	21.3	2.2
+ 0.05 wt% Al_2O_3 NPs	16.5	1.5	17.8	1.4
+ 0.10 wt% Al_2O_3 NPs	11.9	1.1	12.7	1.3
+ 0.15 wt% Al_2O_3 NPs	13.2	1.3	15.0	1.2
+ 0.20 wt% Al_2O_3 NPs	16.4	1.3	18.2	1.5

Elemental mapping and Raman images of the worn surfaces lubricated with the optimal nanolubricant ATF + 0.10 wt% Al_2O_3 NPs were recorded with the confocal Raman microscope to gain insight into the role of NPs in decreasing the worn surface on pins. The Raman spectrum of the Al_2O_3 NPs (Fig. 3) match those obtained by analyzing the worn tracks lubricated with the optimum nanolubricant. Thus, Fig. 10 displays a significant presence of ATF (red color) and significant spots due to Al_2O_3 NPs (blue color) in the mapping of the worn surface lubricated with the optimum nanolubricant. The average size of the Al_2O_3 NPs is very small (5 nm), so they can easily come into the sliding contact.

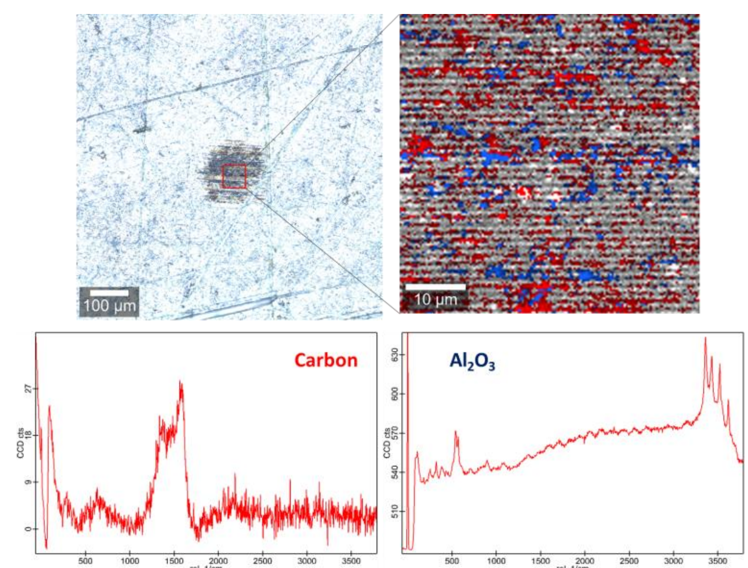

Fig. 10 Raman spectra and elemental mapping of the worn surface tested with the optimal Al_2O_3 nanolubricant.

Regarding the SEM analysis, Fig. 11 shows the worn tracks of the tested pins lubricated with the ATF (Fig. 11a) or with the optimal nanolubricant ATF + 0.10 wt% Al_2O_3 NPs (Fig. 11b) at 5000x. It can be seen that for the worn track lubricated with the optimal nanolubricant the surface is smoother, specifically in Fig. 11a there is a deep elongated groove along the sliding direction, which can be formed as a product of abrasive wear. This agrees with the roughness measurements (Table 2).

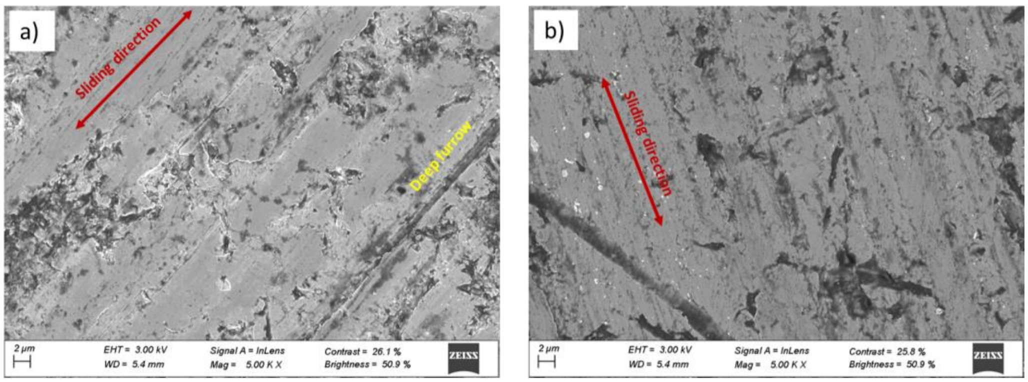

Fig. 11 SEM micrographs of worn surfaces of the tested pins lubricated with a) ATF and b) ATF + 0.10 wt% Al_2O_3 NPs.

The presence of Al_2O_3 NPs on the worn surface of a tested pin lubricated with the optimal nanolubricant was analyzed with EDX, as shown in Fig. 12. The signals detected indicate that Al_2O_3 NPs are deposited and filled into the plow on the worn surface during the tribological tests, with an aluminum (Al) content of 0.9 wt%. Therefore, this fact suggests mending effect where the surface scratch is smoother, and the plow furrow is shallower, reducing both the friction coefficient and wear.

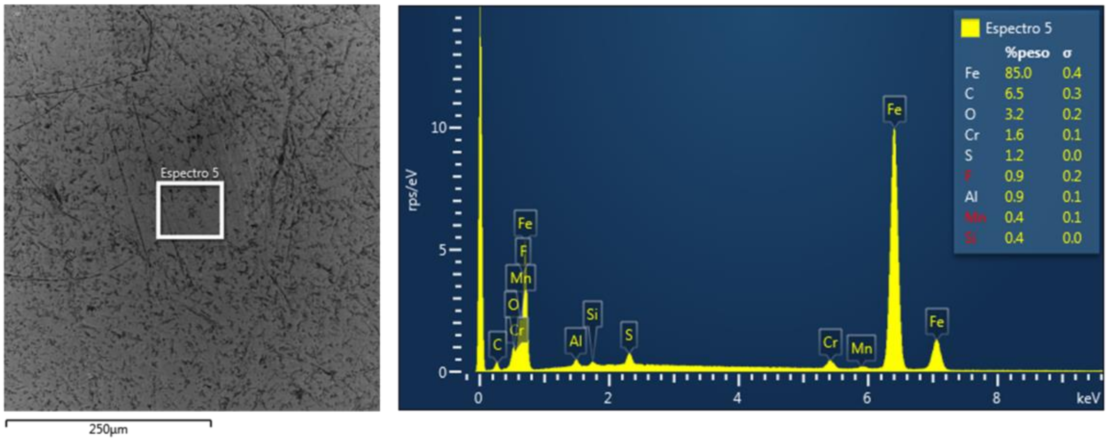

Fig. 12 EDX spectrum of the worn surface of a tested pin lubricated with the optimal nanolubricant.

Finally, due to the high temperature produced by friction and taking into account that tribological tests are performed at 120 ^{o}C, the Al_2O_3 NPs can be chemically adsorbed on the worn surface through hydroxyl groups [42,43] and tribo-sinter to the worn surface, reducing the metal to metal contact [4,44]. Furthermore, Al_2O_3 NPs are mainly spherical (Fig. 1); consequently, the NPs can play the role of ball bearings (known as rolling effect) that avoid the direct contact of the components of the tribological pair, and the sliding friction is shifted to rolling friction improving the extreme pressure behavior and the carrying capability of the nanolubricant [37]. Based on the obtained results, Al_2O_3 NPs used as additives of ATF play an improved anti-friction and anti-wear effect.

Thus, considering all the characterization for describe the possible tribological mechanisms (Roughness, Raman Mapping and SEM-EDX) it can be summarized that these mechanisms can be mending, the tribo-sintering and the rolling effect due to the presence of Al_2O_3 NPs. Therefore, the important improvement achieved mainly in the reduction of wear with respect to the base oil is supported by the appearance of these three important tribological mechanisms.

4. Conclusions

Four low viscosity nanolubricants, which are based on a commercial ATF and containing up to 0.20 wt% of Al_2O_3 NPs, were formulated, achieving temporal stabilities of two weeks. The addition of these NPs enhances the tribological properties of the commercial ATF. Specifically, the best enhancements were found with the ATF + 0.10 wt% of Al_2O_3 nanolubricant: the reductions of the diameter, depth, and transversal area of the worn scar compared to the commercial ATF are 45, 57 and 78%, respectively. For this reason, 0.10 wt% of Al_2O_3 NPs is considered the optimum concentration. The lubrication mechanism can be primarily explained through the mending and the tribo-sintering effects, as revealed by Raman, roughness and SEM-EDX studies of worn surfaces, apart from the rolling effect resulting from the NPs' spherical shape. It is not obvious to evidence this last effect. This result is highly significant because a) the ATF oil is specifically formulated with additive packages for its use as an automatic transmission fluid, and b) it contains optimized anti-wear and anti-friction additives, which have positive synergies with nanomaterials.

CRediT authorship contribution statement

José M. Liñeira del Río: Writing - review & editing, Writing - original draft, Methodology, Investigation, Conceptualization. **Enriqueta R. López:** Writing - review & editing, validation, supervision, formal analysis **Josefa Fernández**: Writing - review & editing, Validation, Supervision, Project administration, Funding acquisition, Conceptualization.

Declaration of competing interest

None

Acknowledgments

This research is supported by Xunta de Galicia (ED431C 2020/10), by MCIN/AEI/10.13039/501100011033 through the PID2020-112846RB-C22 project. JMLdR is grateful for financial support through the Margarita Salas program, funded by MCIN/AEI/10.13039/501100011033 and "NextGenerationEU/PRTR". Furthermore, authors are also grateful to Repsol Lubricants for providing the ATF and to RIAIDT-USC for its analytical facilities.

REFERENCES

[1] K. Holmberg, A. Erdemir, The impact of tribology on energy use and CO_2 emission globally and in combustion engine and electric cars, Tribology International 135 (2019) 389-396. https://doi.org/10.1016/j.triboint.2019.03.024

[2] K. Holmberg, A. Erdemir, Influence of tribology on global energy consumption, costs and emissions, Friction 5 (2017) 263-284. https://doi.org/10.1007/s40544-017-0183-5

[3] A. García Tuero, C. Sanjurjo, N. Rivera, J.L. Viesca, R. González, A. Hernández Battez, Electrical conductivity and tribological behavior of an automatic transmission fluid additised with a phosphonium-based ionic liquid, Journal of Molecular Liquids 367 (2022) 120581. https://doi.org/10.1016/j.molliq.2022.120581

[4] W. Ahmed Abdalglil Mustafa, F. Dassenoy, M. Sarno, A. Senatore, A review on potentials and challenges of nanolubricants as promising lubricants for electric vehicles, Lubrication Science 34 (2022) 1-29. https://doi.org/10.1002/ls.1568

[5] C.C. Y. Kwak, A. Adhvaryu, X. Fang et al., "Understanding Base Oils and Lubricants for Electric Drivetrain Applications," SAE Technical Paper 2019-01-2337, 2019. https://doi.org/10.4271/2019-01-2337.

[6] S. Tung, R. Shah, Global Insights on Future Trends of Hybrid/EV Driveline Lubrication and Thermal Management, Frontiers in Mechanical Engineering 6 (2020) 571786. https://doi.org/10.3389/fmech.2020.571786

[7] K. Narita, D. Takekawa, Lubricants Technology Applied to Transmissions in Hybrid Electric Vehicles and Electric Vehicles, SAE Technical Paper 2019-01-2338 (2019). https://doi.org/10.4271/2019-01-2338.

[8] Z.A.A.A. Ali, A.M. Takhakh, M. Al-Waily, A review of use of nanoparticle additives in lubricants to improve its tribological properties, Materials Today: Proceedings 52 (2022) 1442-1450. https://doi.org/10.1016/j.matpr.2021.11.193

[9] S.C. Tung, M. Woydt, R. Shah, Global Insights on Future Trends of Hybrid/EV Driveline Lubrication and Thermal Management, Frontiers in Mechanical Engineering 6 (2020). https://doi.org/10.3389/fmech.2020.571786

[10] W. Dai, B. Kheireddin, H. Gao, H. Liang, Roles of nanoparticles in oil lubrication, Tribology International 102 (2016) 88-98. https://doi.org/10.1016/j.triboint.2016.05.020

[11] D. Berman, A. Erdemir, A.V. Sumant, Graphene: a new emerging lubricant, Materials Today 17 (2014) 31-42. https://doi.org/10.1016/j.mattod.2013.12.003

[12] G. Paul, S. Shit, H. Hirani, T. Kuila, N.C. Murmu, Tribological behavior of dodecylamine functionalized graphene nanosheets dispersed engine oil nanolubricants, Tribology International 131 (2019) 605-619. https://doi.org/10.1016/j.triboint.2018.11.012

[13] M.K.A. Ali, X. Hou, M.A.A. Abdelkareem, Anti-wear properties evaluation of frictional sliding interfaces in automobile engines lubricated by copper/graphene nanolubricants, Friction 8 (2020) 905-916. https://doi.org/10.1007/s40544-019-0308-0

[14] M. Goodarzi, D. Toghraie, M. Reiszadeh, M. Afrand, Experimental evaluation of dynamic viscosity of ZnO–MWCNTs/engine oil hybrid nanolubricant based on changes in temperature and concentration, Journal of Thermal Analysis and Calorimetry 136 (2019) 513-525. https://doi.org/10.1007/s10973-018-7707-8

[15] J.M. Liñeira del Río, E.R. López, J. Fernández, F. García, Tribological properties of dispersions based on reduced graphene oxide sheets and trimethylolpropane trioleate or PAO 40 oils, Journal of Molecular Liquids 274 (2019) 568-576. https://doi.org/10.1016/j.molliq.2018.10.107

[16] J.M. Liñeira del Río, E.R. López, M. González Gómez, S. Yáñez Vilar, Y. Piñeiro, J. Rivas, D.E.P. Gonçalves, J.H.O. Seabra, J. Fernández, Tribological Behavior of Nanolubricants Based on Coated Magnetic Nanoparticles and Trimethylolpropane Trioleate Base Oil, Nanomaterials 10 (2020) 683. https://doi.org/10.3390/nano10040683

[17] K.I. Nasser, J.M. Liñeira del Río, F. Mariño, E.R. López, J. Fernández, Double hybrid lubricant additives consisting of a phosphonium ionic liquid and graphene nanoplatelets/hexagonal boron nitride nanoparticles, Tribology International 163 (2021) 107189. https://doi.org/10.1016/j.triboint.2021.107189

[18] L. Peña-Parás, J. Taha-Tijerina, L. Garza, D. Maldonado-Cortés, R. Michalczewski, C. Lapray, Effect of CuO and Al_2O_3 nanoparticle additives on the tribological behavior of fully formulated oils, Wear 332-333 (2015) 1256-1261. https://doi.org/10.1016/j.wear.2015.02.038

[19] S. Ghalme, P. Koinkar, Y. Bhalerao, Tribology in Industry Effect of Aluminium Oxide (Al_2O_3) Nanoparticles Addition into Lubricating Oil on Tribological Performance, Tribology in Industry 42 (2020) 494-502. https://doi.org/10.24874/ti.871.04.20.07

[20] T. Luo, X. Wei, H. Zhao, G. Cai, X. Zheng, Tribology properties of Al_2O_3/TiO_2 nanocomposites as lubricant additives, Ceramics International 40 (2014) 10103-10109. https://doi.org/10.1016/j.ceramint.2014.03.181

[21] T.P. Gundarneeya, D.P. Vakharia, Performance analysis of journal bearing operating on nanolubricants with TiO2, CuO and Al2O3 nanoparticles as lubricant additives, Materials Today: Proceedings 45 (2021) 5624-5630. https://doi.org/10.1016/j.matpr.2021.02.350

[22] A. Nabhan, A. Rashed, M. Taha, R. Abouzeid, A. Barhoum, Tribological Performance for Steel–Steel Contact Interfaces Using Hybrid MWCNTs/Al2O3 Nanoparticles as Oil-Based Additives in Engines, Fluids, 2022.

[23] M. Nouri, A.H.M. Isfahani, A. Shirneshan, Effects of Fe2O3 and Al2O3 nanoparticle-diesel fuel blends on the combustion, performance and emission characteristics of a diesel engine, Clean Technologies and Environmental Policy 23 (2021) 2265-2284. https://doi.org/10.1007/s10098-021-02134-8

[24] K. Suthar, Y. Singh, A.R. Surana, V.H. Rajubhai, A. Sharma, Experimental evaluation of the friction and wear of jojoba oil with aluminium oxide (Al2O3) nanoparticles as an additive, Materials Today: Proceedings 25 (2020) 699-703. https://doi.org/10.1016/j.matpr.2019.08.150

[25] X. Bai, J. Jiang, C. Li, L. Dong, H.M. Ali, S. Sharma, Tribological Performance of Different Concentrations of Al2O3 Nanofluids on Minimum Quantity Lubrication Milling, Chinese Journal of Mechanical Engineering 36 (2023) 11. https://doi.org/10.1186/s10033-022-00830-0

[26] M.K.A. Ali, H. Xianjun, L. Mai, C. Qingping, R.F. Turkson, C. Bicheng, Improving the tribological characteristics of piston ring assembly in automotive engines using Al2O3 and TiO2 nanomaterials as nano-lubricant additives, Tribology International 103 (2016) 540-554. https://doi.org/10.1016/j.triboint.2016.08.011

[27] J. Saniger, Al-O infrared vibrational frequencies of γ-alumina, Materials Letters 22 (1995) 109-113. https://doi.org/10.1016/0167-577X(94)00234-7

[28] K. Atrak, A. Ramazani, S. Taghavi Fardood, Green synthesis of amorphous and gamma aluminum oxide nanoparticles by tragacanth gel and comparison of their photocatalytic activity for the degradation of organic dyes, Journal of Materials Science: Materials in Electronics 29 (2018) 8347-8353. https://doi.org/10.1007/s10854-018-8845-2

[29] A. Afkhami, M. Saber-Tehrani, H. Bagheri, Simultaneous removal of heavy-metal ions in wastewater samples using nano-alumina modified with 2,4-dinitrophenylhydrazine, Journal of Hazardous Materials 181 (2010) 836-844. https://doi.org/10.1016/j.jhazmat.2010.05.089

[30] M. Baronskiy, A. Rastorguev, A. Zhuzhgov, A. Kostyukov, O. Krivoruchko, V. Snytnikov, Photoluminescence and Raman spectroscopy studies of low-temperature γ-Al_2O_3 phases

synthesized from different precursors, Optical Materials 53 (2016) 87-93. https://doi.org/10.1016/j.optmat.2016.01.029

[31] P.V. Thomas, V. Ramakrishnan, V.K. Vaidyan, Oxidation studies of aluminum thin films by Raman spectroscopy, Thin Solid Films 170 (1989) 35-40. https://doi.org/10.1016/0040-6090(89)90619-6

[32] J. Läuger, K. Pondicherry, New Insights into the Use of a Rotational Rheometer as Tribometer (2017).

[33] P. Heyer, J. Läuger, Correlation between friction and flow of lubricating greases in a new tribometer device, 21 (2009) 253-268. https://doi.org/10.1002/ls.88

[34] K.I. Nasser, J.M. Liñeira del Río, E.R. López, J. Fernández, Synergistic effects of hexagonal boron nitride nanoparticles and phosphonium ionic liquids as hybrid lubricant additives, Journal of Molecular Liquids 311 (2020) 113343. https://doi.org/10.1016/j.molliq.2020.113343

[35] E. Rodríguez, N. Rivera, A. Fernández-González, T. Pérez, R. González, A.H. Battez, Electrical compatibility of transmission fluids in electric vehicles, Tribology International 171 (2022) 107544. https://doi.org/10.1016/j.triboint.2022.107544

[36] N. Han, R. Kim, H. Lee, T. Beom, Y. Kim, D. Kim, Analysis of flow field in the motor-reducer assembly with oil cooling under real driving conditions, Journal of Mechanical Science and Technology 37 (2023) 1539-1550. https://doi.org/10.1007/s12206-023-0239-6

[37] T. Luo, X. Wei, X. Huang, L. Huang, F. Yang, Tribological properties of Al_2O_3 nanoparticles as lubricating oil additives, Ceramics International 40 (2014) 7143-7149. https://doi.org/10.1016/j.ceramint.2013.12.050

[38] N.A. Ismail, S. Bagheri, Highly oil-dispersed functionalized reduced graphene oxide nanosheets as lube oil friction modifier, Materials Science and Engineering: B 222 (2017) 34-42. https://doi.org/10.1016/j.mseb.2017.04.010

[39] V. Zin, S. Barison, F. Agresti, L. Colla, C. Pagura, M. Fabrizio, Improved tribological and thermal properties of lubricants by graphene based nano-additives, RSC Advances 6 (2016) 59477-59486. https://doi.org/10.1039/C6RA12029F

[40] L. Liu, Z. Fang, A. Gu, Z. Guo, Lubrication Effect of the Paraffin Oil Filled with Functionalized Multiwalled Carbon Nanotubes for Bismaleimide Resin, Tribology Letters 42 (2011) 59-65. https://doi.org/10.1007/s11249-011-9749-y

[41] W. Li, S. Zheng, B. Cao, S. Ma, Friction and wear properties of ZrO2/SiO2 composite nanoparticles, Journal of Nanoparticle Research 13 (2011) 2129-2137. https://doi.org/10.1007/s11051-010-9970-x

[42] M. Kobayashi, R. Matsuno, H. Otsuka, A. Takahara, Precise surface structure control of inorganic solid and metal oxide nanoparticles through surface-initiated radical polymerization, Science and Technology of Advanced Materials 7 (2006) 617-628. https://doi.org/10.1016/j.stam.2006.07.008

[43] G. Liu, X. Li, B. Qin, D. Xing, Y. Guo, R. Fan, Investigation of the Mending Effect and Mechanism of Copper Nano-Particles on a Tribologically Stressed Surface, Tribology Letters 17 (2004) 961-966. https://doi.org/10.1007/s11249-004-8109-6

[44] A. Hernández Battez, J.L. Viesca, R. González, D. Blanco, E. Asedegbega, A. Osorio, Friction reduction properties of a CuO nanolubricant used as lubricant for a NiCrBSi coating, Wear 268 (2010) 325-328. https://doi.org/10.1016/j.wear.2009.08.018